Waves in Random and Complex Media

ISSN: (Print) (Online) Journal homepage: https://www.tandfonline.com/loi/twrm20

Advance thermal and mass transports for the fractional flows through a cylindrical domain: a Prabhakar-like generalization

Zaib Un Nisa, Muhammad Asad Meraj, Ahmad Shafique, Mushtaq Ahmad, Mudassar Nazar & Nehad Ali Shah

WAVES IN RANDOM AND COMPLEX MEDIA
https://doi.org/10.1080/17455030.2022.2154408

Advance thermal and mass transports for the fractional flows through a cylindrical domain: a Prabhakar-like generalization

Zaib Un Nisa[a,†], Muhammad Asad Meraj[a], Ahmad Shafique[b], Mushtaq Ahmad[b,c], Mudassar Nazar[b,d] and Nehad Ali Shah[e†]

[a]Department of Mathematics, University of Education Lahore, Multan, Pakistan; [b]Centre for Advanced Studies in Pure and Applied Mathematics, Bahauddin Zakariya University, Multan, Pakistan; [c]Department of Mathematics & Statistics Institute of Southern Punjab, Multan, Pakistan; [d]School of Mathematical Sciences, University of Science and Technology of China, Hefei, People's Republic of China; [e]Department of Mechanical Engineering, Sejong University, Seoul, South Korea

ABSTRACT

In this study, the flow of a viscous fluid through an infinite vertical cylinder is discussed. The respective flow is induced by pressure gradient and with the contribution of temperature and concentration gradients. The flow modeling is done with the generalized heat and molecular fluxes by utilizing the Prabhakar-like fractional derivative. The fractional partial differential equations which govern the flow model are reduced to the dimensionless form to project the deep understanding of the flow model and then solved analytically by integral transforms namely Hankel and Laplace transforms. The physical aspects of flow regarding involved parameters especially fractional parameter are discussed by sketching the graphs of field variables for the concerned parametric variations.

ARTICLE HISTORY
Received 21 February 2022
Accepted 21 November 2022

KEYWORDS
Free convection flow; cylindrical domain; heat and mass transfer; Prabhakar-like fractional derivative; Hankel transform

1. Introduction

The free convection flow with thermal and mass transfers through a closed circular domain like cylinder has earned the significant attention due to its applications in biological sciences, industries, and important relevancy on several technological processes. Jamil et al. [1] discussed two-dimensional flow of rate type fluid in cylindrical domain. Mehmood et al. [2] obtained the closed-form results for the generalized cylindrical flow of non-Newtonian fluid. Awan et al. [3] investigated cylindrical flow along the axis of cylinder. Maryam et al. [4] discussed the flow of viscous fluid a channel. Nazar et al. [5, 6] considered an unsteady flow of differential-type fluid in closed domain. Tong et al. [7] investigated the result for generalized Burger's fluid in an annular pipe. Shaowei et al. [8] established the results for natural convection flow of viscous fluid through a vertical cylinder. Gul et al. [9] worked on free convection flows of blood with the Marangoni convection and magnetic field. The study of

CONTACT Nehad Ali Shah nehadali199@yahoo.com
† Zaib Un Nisa and Nehad Ali Shah are contributed equally to this work and are co-first authors.

the derivative of arbitrary order is known as the fractional calculus and it has become a fertile field of science and engineering [10–12]. Elnaqeeb et al. [13] discussed the generalized thermal transport for the flow of nanofluid with Prabhakar-like fractional derivative.

Shah et al. [14] considered the damping effect on convective flows through vertical cylinder. Prakash and Ogulu [15] discussed the blood flow in constricted tubes. Saqib et al. [16] considered MHD blood flow with fractional derivative. Imran et al. [17] also considered the fractional approach to discuss the flow of rate type fluid in the annulus of two concentric cylinders. Some other interesting cylindrical flows with fractional derivatives are presented in [18–30]. In this work, the flow of viscous fluid through a cylindrical domain is discussed by utilizing the Prabhakar-like fractional derivative. Closed-form results for temperature, concentration, and velocity fields are established with the help of integral transforms namely Hankel and Laplace transformations. Also the effect of fractional parameter and flow parameters is investigated by plotting graphically.

2. Mathematical formulation

Suppose a vertical cylinder of the infinite length and radius 'r_0' is lying along the z-axis as drawn in Figure 1. The flow of viscous fluid is assumed to be in the z-direction and double convection flow is induced by the pressure gauge and bouncy effect. The radial direction is taken normal to the axis of the cylinder as well as the flow direction. For time $t \leq 0$, the cylinder and filled fluid both are in state of rest and thermal state and concentration level of the system are prescribed by T_∞ and C_∞ respectively. For $t > 0$, the heat transfer takes place from the curved surface of cylinder to the fluid and temperature of fluid rises from T_∞ to constant value T_w while concentration level reaches to C_w. The mathematical form of cylindrical flow model is described in the following partial differential equations [23]:

$$\rho \frac{\partial u}{\partial t} = \mu \left(\frac{\partial^2 u(r,t)}{\partial r^2} + r^{-1} \frac{\partial u(r,t)}{\partial r} \right) - \frac{\partial p}{\partial z} + \rho g \beta_T [T(r,t) - T_\infty] - \rho g \beta_C [C(r,t) - C_\infty]. \quad (1)$$

The periodic pressure is given by in term of amplitude pressures [24]

$$-\frac{\partial p}{\partial z} = \rho_\circ + \rho_1 \cos(\omega t), \quad (2)$$

where $\rho_\circ$ and ρ_1 are the amplitude values of pressure known as systolic and diastolic pressures [24, 25].

Heat energy balance equation is

$$-\frac{\partial q(r,t)}{\partial r} + r^{-1} q(r,t) = \rho c_p \frac{\partial T(r,t)}{\partial t}. \quad (3)$$

Fourier's law for transport of heat

$$q(r,t) = -k \frac{\partial T(r,t)}{\partial r}. \quad (4)$$

Molecular diffusion equation is

$$\frac{\partial C(r,t)}{\partial t} = -\frac{\partial J(r,t)}{\partial r} + \frac{1}{r} J(r,t), \quad (5)$$

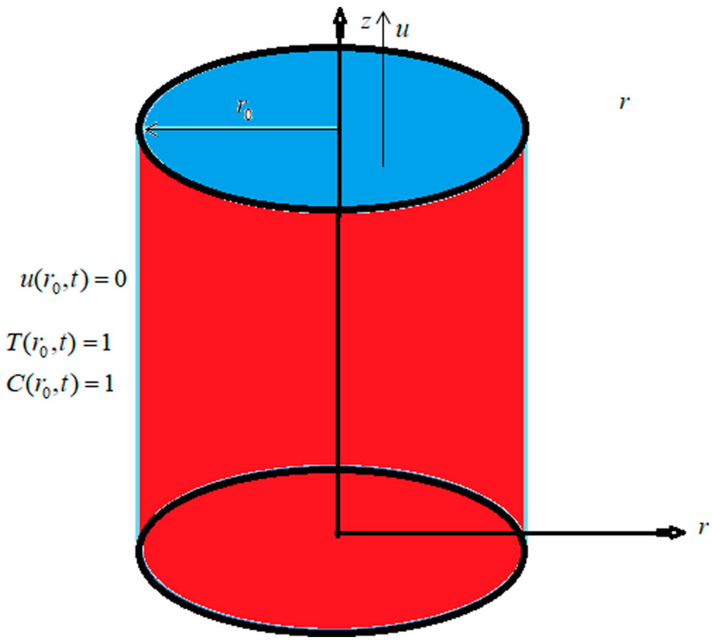

Figure 1. Flow model and geometry.

Fick's law for molecular transport

$$J(r,t) = -D\frac{\partial C(r,t)}{\partial r}. \tag{6}$$

Specified values of temperature at $t = 0$ and at boundary of flow domain are given by

$$u(r,0) = 0,\ T(r,0) = T_\infty,\ C(r,0) = C_\infty,\ r \in [0, r_0], \tag{7}$$

$$u(r_0,t) = 0,\ T(r_0,t) = T_w,\ C(r_0,t) = C_w,\ t > 0. \tag{8}$$

Introducing the following relations to get the shape free model:

$$\acute{r} = \frac{r}{r_0},\ \acute{u} = \frac{u}{U_0},\ \acute{t} = \frac{t\nu}{r_0^2},\ \chi = \frac{T - T_\infty}{T_w - T_\infty},\ \phi = \frac{C - C_\infty}{C_w - C_\infty},\acute{q} = \frac{qr_0}{k(T_w - T_\infty)},$$
$$\acute{J} = \frac{Jr_0}{D(T_w - T_\infty)},\acute{\rho}_0 = \frac{\rho_0 r_0^2}{\nu\rho U_0},\acute{\rho}_1 = \frac{\rho_1 r_0^2}{\nu\rho U_0}, \tag{9}$$

and after unhanding the prime notation we get

$$\frac{\partial u}{\partial t} = \left(\frac{\partial^2 u(r,t)}{\partial r^2} + \frac{1}{r}\frac{\partial u(r,t)}{\partial r}\right) + \rho_\circ + \rho_1\cos(ft) + \mathrm{Gr}\chi(r,t) - \mathrm{Gm}\phi(r,t), \tag{10}$$

where $\mathrm{Gr} = \frac{g\beta_T(T_w - T_\infty)}{U_0^3}$, $\mathrm{Gm} = \frac{g\beta_C(C_w - C_\infty)}{U_0^3}$.

Non-dimensional heat energy balance equation is

$$\mathrm{Pr}\frac{\partial \chi(r,t)}{\partial t} = -\left(\frac{\partial q(r,t)}{\partial r} + \frac{1}{r}q(r,t)\right), \tag{11}$$

Fourier's law in dimensionless form

$$q(r,t) = -\frac{\partial \chi(r,t)}{\partial r}. \tag{12}$$

Non-dimensional molecular diffusion equation is

$$\mathrm{Sc}\frac{\partial \phi(r,t)}{\partial t} = -\frac{\partial J(r,t)}{\partial r} + \frac{1}{r}J(r,t), \tag{13}$$

and Fick's law in dimensionless form

$$J(r,t) = -\frac{\partial \phi(r,t)}{\partial r}, \tag{14}$$

where $\mathrm{Pr} = \frac{\mu C_p}{k}$ and $\mathrm{Sc} = \frac{\nu}{D}$ are thermal and mass Prandtl numbers with following dimensionless specified values of field variables.

$$u(r,0) = 0,\ T(r,0) = 0,\ C(r,0) = 0,\ r\ \in [0,1] \tag{15}$$

$$u(1,t) = 0,\ T(1,t) = 1,\ C(1,t) = 1,\ t > 0. \tag{16}$$

2.1. Generalized heat and mass transports

The Fourier's and Fick's laws with fractional derivatives are stated as

$$q(r,t) = -D^{\gamma}_{\alpha,\beta,a}\frac{\partial \chi(r,t)}{\partial r} \tag{17}$$

and

$$J(r,t) = -D^{\gamma}_{\alpha,\beta,a}\frac{\partial \phi(r,t)}{\partial r}, \tag{18}$$

where

$$D^{\gamma}_{\alpha,\beta,a}f(r,t) = \int_0^t (t-\tau)^{n-\beta+1}E^{\gamma}_{\alpha,n-\beta}[a(t-\tau)^{\alpha}]\frac{d^n f(r,t)}{dt^n} \tag{19}$$

is the Prabhakar's fractional derivative. The Laplace transformation of Prabhakar fractional derivatives is below [13]

$$L\left\{D^{\gamma}_{\alpha,\beta,a}f(r,t)\right\} = p^{\beta-n}(1-ap^{\alpha})^{\gamma}L\{\frac{d^n f(r,t)}{dt^n}\}. \tag{20}$$

3. Solution of problem

The fractional flow model is solved by Laplace transform [31, 32].

3.1. Temperature field

Equations (11), $(16)_2$ and (17) under the Laplace transform, for $n = 0$, get the following form:

$$\mathrm{Pr}p\bar{\chi}(r,p) = -\left(\frac{\partial\bar{q}(r,p)}{\partial r} + r^{-1}\bar{q}(r,p)\right), \tag{21}$$

$$\bar{q}(r,p) = -p^{\beta}(1-ap^{\alpha})^{\gamma}\frac{\partial\bar{\chi}(r,p)}{\partial r}, \tag{22}$$

$$\bar{\chi}(1,p) = \frac{1}{p}. \tag{23}$$

Now using Equation (22) in Equation (21), we get

$$\left(\frac{\partial^2}{\partial r^2} + \frac{1}{r}\frac{\partial}{\partial r}\right)\bar{\chi}(r,p) = \frac{\mathrm{Pr}p}{p^{\beta}(1-ap^{-\alpha})^{\gamma}}\bar{\chi}(r,p), \tag{24}$$

where p is the Laplace parameter and the function $\bar{\chi}(r,p)$ is Laplace image of $\chi(r,p)$. Now applying the Hankel transform [33] keeping in mind the transformed condition $\bar{\chi}(1,p) = \frac{1}{p}$

$$\bar{\chi}_H(r_n,p) = \frac{r_nJ_1(r_n)}{p}\frac{p^{\beta}(1-ap^{-\alpha})^{\gamma}}{r_n^2p^{\beta}(1-ap^{-\alpha})^{\gamma} + \mathrm{Pr}p}. \tag{25}$$

Equivalently can be written as

$$\bar{\chi}_H(r_n,p) = \frac{J_1(r_n)}{r_n}\frac{1}{p} - \frac{J_1(r_n)}{r_n}\frac{\mathrm{Pr}}{r_n^2p^{\beta}(1-ap^{-\alpha})^{\gamma} + \mathrm{Pr}p}. \tag{26}$$

In summation

$$\bar{\chi}_H(r_n,p) = \frac{J_1(r_n)}{r_n}\frac{1}{p} - \frac{J_1(r_n)}{r_n}\sum_{l=0}^{\infty}\sum_{m=0}^{\infty}(-)^l(\mathrm{Pr}_1)^l(-a)^m\frac{\Gamma(\gamma l+1)}{\Gamma(\gamma l+1-m)\Gamma(1+m)} \times \frac{1}{p^{2-l(\beta-1)+\alpha m}}, \tag{27}$$

where $\mathrm{Pr}_1 = \frac{r_2^2}{\mathrm{Pr}}$.

Applying inverse Laplace transform

$$\chi_H(r_n,t) = \frac{J_1(r_n)}{r_n} - \frac{J_1(r_n)}{r_n}\sum_{l=0}^{\infty}\sum_{m=0}^{\infty}\frac{(-)^l(\mathrm{Pr}_1)^l(-a)^m\Gamma(1+\gamma l)}{\Gamma(m+1)\Gamma(\gamma l+1-m)}\frac{t^{1-l(\beta-1)+m\alpha}}{\Gamma(1-l(\beta-1)+\alpha m)}. \tag{28}$$

Applying inverse Hankel transformation

$$\chi(r,t) = 1 - 2\sum_{n=1}^{\infty}\sum_{l=0}^{\infty}\sum_{m=0}^{\infty}\frac{J_0(r_nr)}{r_nJ_1(r_n)}\frac{(-)^l(\mathrm{Pr}_1)^l(-a)^m\Gamma(\gamma l+1)}{\Gamma(m+1)\Gamma(\gamma l-m+1)}\frac{t^{1-l(\beta-1)+\alpha m}}{\Gamma(1-l(\beta-1)+\alpha m)}. \tag{29}$$

3.2. Concentration field

Equations (13), $(16)_3$ and (18) for $n = 0$, and under the Laplace transform take the following form:

$$\mathrm{Sc}p\bar{\phi}(r,p) = -\left(\frac{\partial \bar{J}(r,p)}{\partial r} + \frac{1}{r}\bar{J}(r,q)\right), \tag{30}$$

$$\bar{J}(r,p) = -p^{\beta}(1-ap^{\alpha})^{\gamma}\frac{\partial \bar{\phi}(r,p)}{\partial r}, \tag{31}$$

$$\bar{\phi}(1,p) = \frac{1}{p}. \tag{32}$$

Now using Equation (31) in Equation (30), we get

$$\left(\frac{\partial^2}{\partial r^2} + \frac{1}{r}\frac{\partial}{\partial r}\right)\bar{\phi}(r,p) = \frac{\mathrm{Sc}p}{p^{\beta}(1-ap^{-\alpha})^{\gamma}}\bar{\phi}(r,p), \tag{33}$$

where the function $\bar{\phi}(r,p)$ is Laplace image of $\phi(r,p)$. Now applying the Hankel transform, keeping in mind the transformed condition $\bar{\phi}(1,p) = \frac{1}{p}$

$$\bar{\phi}_H(r_n,p) = \frac{r_nJ_1(r_n)}{p}\frac{p^{\beta}(1-ap^{-\alpha})^{\gamma}}{r_n^2p^{\beta}(1-ap^{-\alpha})^{\gamma} + \mathrm{Sc}p}. \tag{34}$$

Equivalently can be written as

$$\bar{\phi}_H(r_n,p) = \frac{J_1(r_n)}{r_n}\frac{1}{p} - \frac{J_1(r_n)}{r_n}\frac{\mathrm{Pr}}{r_n^2p^{\beta}(1-ap^{-\alpha})^{\gamma} + Scp}. \tag{35}$$

In summation

$$\bar{\phi}_H(r_n,p) = \frac{J_1(r_n)}{r_n}\frac{1}{p} - \frac{J_1(r_n)}{r_n}\sum_{l=0}^{\infty}\sum_{m=0}^{\infty}(-1)^l(\mathrm{Sc}_1)^l(-a)^m\frac{\Gamma(\gamma l+1)}{\Gamma(m+1)\Gamma(\gamma l-m+1)} \times \frac{1}{p^{2-l(\beta-1)+\alpha m}}, \tag{36}$$

where $\mathrm{Sc}_1 = \frac{r_2^2}{\mathrm{Sc}}$.

Applying inverse Laplace transform transformation

$$\phi_H(r_n,t) = \frac{J_1(r_n)}{r_n} - \frac{J_1(r_n)}{r_n}\sum_{l=0}^{\infty}\sum_{m=0}^{\infty}\frac{(-1)^l(\mathrm{Sc}_1)^l(-a)^m\Gamma(\gamma l+1)}{\Gamma(m+1)\Gamma(\gamma l-m+1)}\frac{t^{1-l(\beta-1)+\alpha m}}{\Gamma(1-l(\beta-1)+\alpha m)}. \tag{37}$$

Applying inverse Hankel transformation

$$\phi(r,t) = 1 - 2\sum_{n=1}^{\infty}\sum_{l=0}^{\infty}\sum_{m=0}^{\infty}\frac{J_0(r_nr)}{r_nJ_1(r_n)}\frac{(-1)^l(\mathrm{Sc}_1)^l(-a)^m\Gamma(\gamma l+1)}{\Gamma(m+1)\Gamma(\gamma l-m+1)}\frac{t^{1-l(\beta-1)+\alpha m}}{\Gamma(1-l(\beta-1)+\alpha m)}. \tag{38}$$

3.3. Velocity field

Equation (9) under Laplace transform with its relative initial condition takes the following form:

$$p\bar{u}(r,p) = \left(\frac{\partial^2\bar{u}(r,q)}{\partial r^2} + \frac{1}{r}\frac{\partial\bar{u}(r,p)}{\partial r}\right) + \frac{\rho_\circ}{p} + \frac{\rho_1 p}{p^2+f^2} + \mathrm{Gr}\bar{\chi}(r,p) + \mathrm{Gm}\bar{\phi}(r,p), \tag{39}$$

which satisfies the following condition:

$$\bar{u}(1,p) = 0. \tag{40}$$

Applying the Hankel transform

$$p\bar{u}_H(r_n,p) = -r_n^2\bar{u}_H(r_n,p) + \frac{J_1(r_n)}{r_n}\left(\frac{\rho_\circ}{p} + \frac{\rho_1 p}{p^2+f^2}\right) + \mathrm{Gr}\bar{\chi}(r,p) + \mathrm{Gm}\bar{\phi}(r,p), \tag{41}$$

and coupling the expression of $\bar{\chi}_H(r_n,p)$ and $\bar{\phi}_H(r_n,p)$ from Equations (20) and (26) in Equation (31), we get

$$\begin{aligned}\bar{u}_H(r_n,p) &= \frac{J_1(r_n)}{r_n}\frac{1}{(p+r_n^2)}\left(\frac{\rho_\circ}{p} + \frac{\rho_1 p}{p^2+f^2}\right)\\ &\quad + \mathrm{Gr}\frac{r_nJ_1(r_n}{(p+r_n^2)}\left[\frac{1}{p}\frac{\mathrm{Pr}p^\beta(1-ap^{-\alpha})^\gamma}{r_n^2p^\beta(1-ap^{-\alpha})^\gamma + \mathrm{Pr}p}\right]\\ &\quad + \mathrm{Gm}\frac{r_nJ_1(r_n)}{(p+r_n^2)}\left[\frac{1}{p}\frac{\mathrm{Sc}p^\beta(1-ap^{-\alpha})^\gamma}{r_n^2p^\beta(1-ap^{-\alpha})^\gamma + Scp}\right].\end{aligned} \tag{42}$$

In summation notation

$$\begin{aligned}\bar{u}_H(r_n,p) &= \frac{J_1(r_n)}{r_n}\frac{1}{(p+r_n^2)}\left(\frac{\rho_\circ}{p} + \frac{\rho_1 p}{p^2+f^2}\right)\\ &\quad + \frac{\mathrm{Gr}J_1(r_n)}{r_n(p+r_n^2)}\sum_{l=0}^{\infty}\sum_{m=0}^{\infty}(-1)^l(\mathrm{Pr}_1)^{-l}(-a)^m\frac{\Gamma(\gamma l+1)}{\Gamma(m+1)\Gamma(\gamma l-m+1)}\frac{1}{p^{1-l(\beta-1)+\alpha m}}\\ &\quad + \frac{\mathrm{Gm}J_1(r_n)}{r_n(p+r_n^2)}\sum_{l=0}^{\infty}\sum_{m=0}^{\infty}(-1)^l(\mathrm{Sc}_1)^{-l}(-a)^m\\ &\quad \times\frac{\Gamma(\gamma l+1)}{\Gamma(m+1)\Gamma(\gamma l-m+1)}\frac{1}{p^{1-l(\beta-1)+\alpha m}}.\end{aligned} \tag{43}$$

Now applying the inverse Laplace transform

$$
\begin{aligned}
u_H(r_n,t) = {} & \frac{J_1(r_n)}{r_n}\mathrm{e}^{-r_n^2} * (\rho_\circ + \rho_1\cos(ft)) \\
& + \frac{\mathrm{Gr}J_1(r_n)}{r_n}\mathrm{e}^{-r_n^2} * \sum_{l=0}^{\infty}\sum_{m=0}^{\infty}(-1)^l(\mathrm{Pr}_1)^{-l}(-a)^m \\
& \times \frac{\Gamma(\gamma l+1)}{\Gamma(m+1)\Gamma(\gamma l-m+1)}\frac{t^{\alpha m-l(\beta-1)}}{\Gamma(\alpha m-l(\beta-1))} \\
& + \frac{\mathrm{Gm}J_1(r_n)}{r_n}\mathrm{e}^{-r_n^2} * \sum_{l=0}^{\infty}\sum_{m=0}^{\infty}(-1)^l(\mathrm{Sc}_1)^{-l}(-a)^m \\
& \times \frac{\Gamma(\gamma l+1)}{\Gamma(m+1)\Gamma(\gamma l-m+1)}\frac{t^{-l(\beta-1)+\alpha m}}{\Gamma(\alpha m-l(\beta-1))}.
\end{aligned}
\tag{44}
$$

Inverting Hankel transform

$$
\begin{aligned}
u(r,t) = {} & 2\sum_{n=1}^{\infty}\frac{J_0(r_n r)}{r_n J_1(r_n)}e^{-r_n^2} * (\rho_\circ + \rho_1\cos(ft)) \\
& + 2\mathrm{Gr}\sum_{n=1}^{\infty}\frac{J_0(r_n r)}{r_n J_1(r_n)}e^{-r_n^2} * \sum_{l=0}^{\infty}\sum_{m=0}^{\infty}\frac{(-1)^l(\mathrm{Pr}_1)^{-l}(-a)^m\Gamma(\gamma l+1)}{\Gamma(m+1)\Gamma(\gamma l-m+1)}\frac{t^{-l(\beta-1)+\alpha m}}{\Gamma(\alpha m-l(\beta-1))} \\
& + 2\mathrm{Gm}\sum_{n=1}^{\infty}\frac{J_0(r_n r)}{r_n J_1(r_n)}e^{-r_n^2} * \sum_{l=0}^{\infty}\sum_{m=0}^{\infty}\frac{(-1)^l(\mathrm{Sc}_1)^{-l}(-a)^m\Gamma(1+\gamma l)}{\Gamma(1+m)\Gamma(\gamma l+1-m)}\frac{t^{-l(\beta-1)+\alpha m}}{\Gamma(\alpha m-l(\beta-1))}.
\end{aligned}
\tag{45}
$$

4. Results and discussion

In this work, the flow of a viscous fluid through an infinite vertical cylinder is discussed. The respective flow is induced by pressure gradient and with the contribution of temperature and concentration gradients. The flow modeling is done with the generalized heat and molecular fluxes by utilizing the Prabhakar-like fractional derivative. The respective governing equations of flow model are also reduced to the dimensionless form to project the deep understanding of the flow model and then solved analytically by integral transforms namely Hankel and Laplace transforms. The physical aspects of flow regarding involved parameters especially fractional parameter are discussed by sketching the graphs of field variables for the concerned parametric variations and presented in Figures (2)–(9).

The outcomes of fractional parameter β are posted over the temperature field in Figures 2(a) and 2(b) for short and long times. For short times, temperature profiles presented a growing trend while it has a decaying trend for long times. This adverse behavior of the temperature profile for short and large times is due to the choice of Mittag–Leffler function. The deportment of fractional parameter γ on temperature profile is discussed in Figures 3(a)–3(b) for short and long times, temperature profiles show a decaying trend for both times. This physical aspect of temperature against fractional parameters is due to

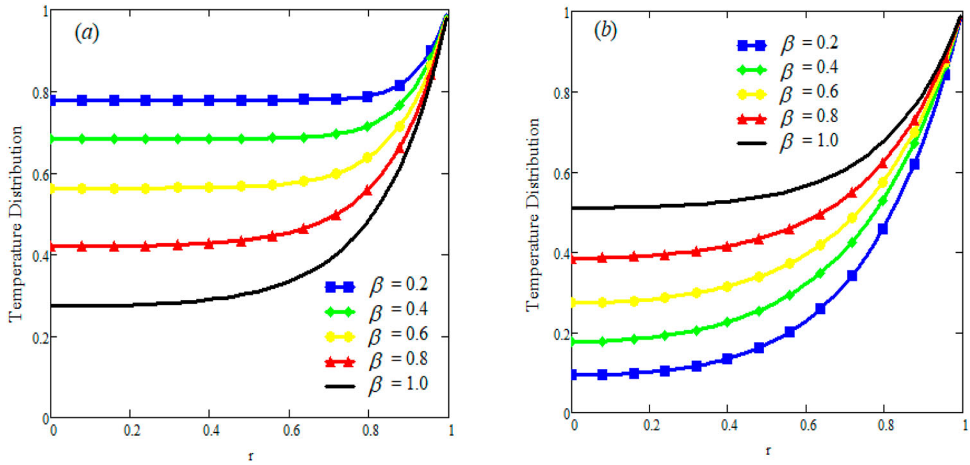

Figure 2. Temperature profile due to the variation of β for times $t = 0.2$ and $t = 2$.

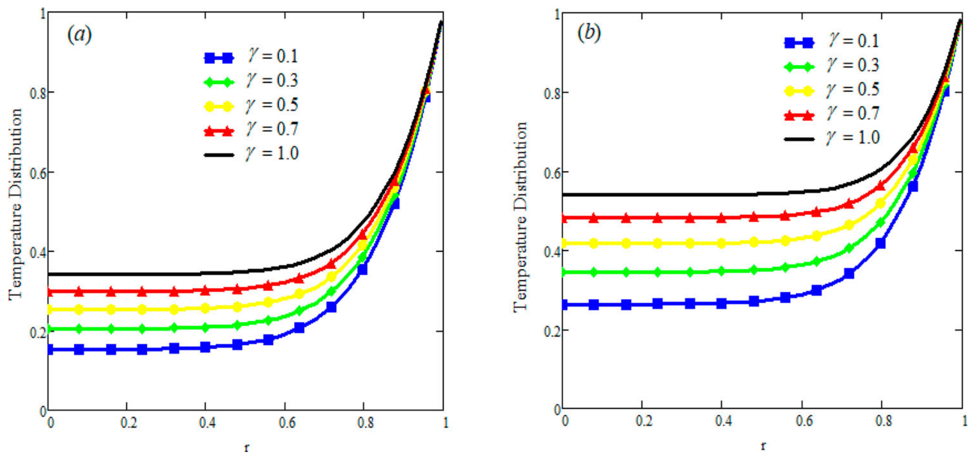

Figure 3. Temperature profile due to the variation of γ for times $t = 0.2$ and $t = 2$.

the choice of the generalized three-parametric Mittag–Leffler function as a kernel of fractional operator. The same behavior of concentration against the corresponding parameters is appeared in Figures (4) and (5).

In Figures 6(a) and 6(b), the velocity profile is plotted for due variation of fractional parameter β. Velocity profiles also present an adverse behavior for short and long times. From the figures it is cleared the velocity profile is an increasing function for short time while it is a decreasing function for large time and reason behind such behavior is the Mittag–Leffler kernel for fractional operator. Velocity field is sketched for fractional parameter γ in Figures 7(a) and 7(b) and it is noted a decreasing trend in velocity profile for increasing values of γ. The effect of Gr and Gm is discussed in Figures 8(a) and 8(b). From the sketches of profiles, it is observed that velocity field post an increasing trend for increasing values of Gr and Gm. Gr and Gm are the ratio of bouncy forces due to temperature gradient and mass gradient restively to the viscous force. Larger the value of Gr and Gm larger the

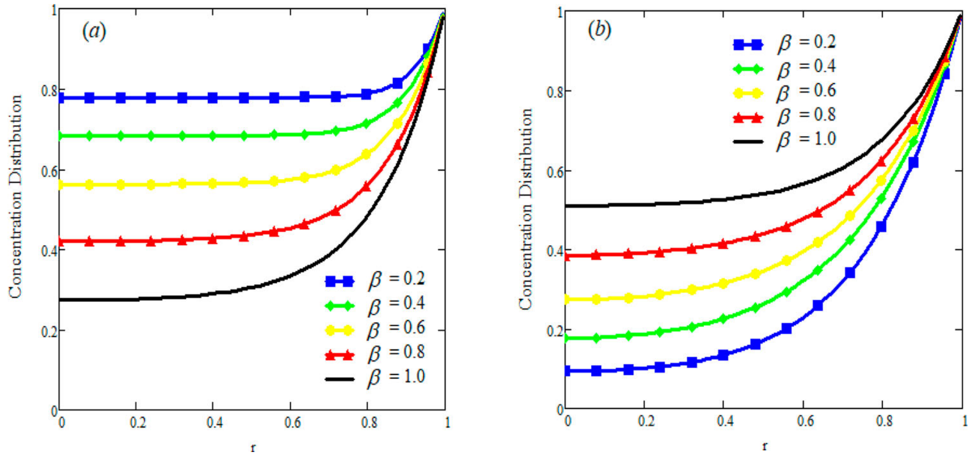

Figure 4. Temperature profile due to the variation of β for times $t = 0.2$ and $t = 2$.

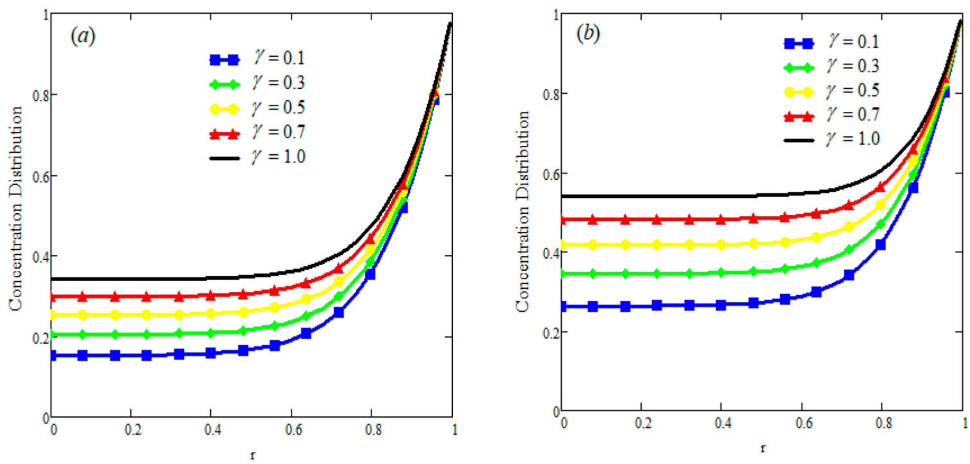

Figure 5. Temperature profile due to the variation of γ for times $t = 0.2$ and $t = 2$.

bouncy effect therefore fluid speeds up for increasing values of Gr and Gm. The physical reasoning behind this increasing trend is that for larger values of both Gr and Gm there are more buoyancy forces which always support the fluid velocity so fluid speeds up with increasing values of Gr and Gm. The physical effect of thermal Prandtl number Pr and mass Prandtl numbers Sc is highlighted in Figures 9(a) and 9(b) and the falling curves appeared for the increasing values of Pr and Sc. As Pr and Sc are the ratio of momentum diffusivity to the thermal and molecular diffusivities respectively. Larger the values of Pr and Sc, there is more momentum diffusivity and more viscous friction in the fluid domain which reduces the velocity of fluid and boundary layer thickness too. In Figure 10(a), comparison of the present velocity for $\alpha, \beta \rightarrow 1$ with that velocity obtained by Nazar et al. [5]. From the figure it is observed that the overlapping profiles show the validity of our obtained results.

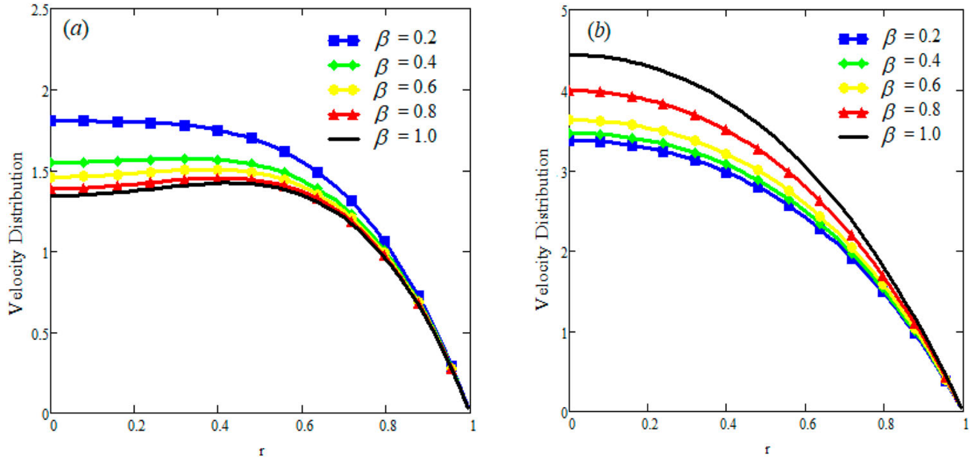

Figure 6. Velocity profile due to the variation of β for times $t = 0.2$ and $t = 2$.

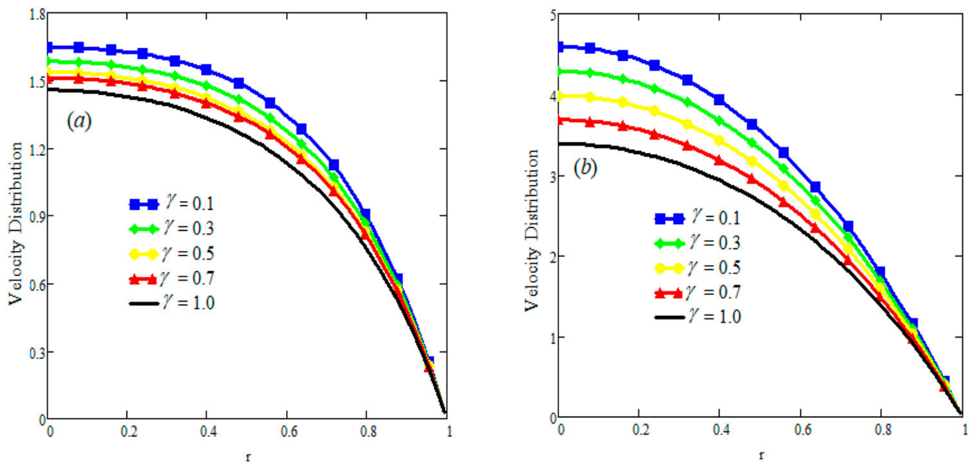

Figure 7. Velocity profile due to variation of γ for times $t = 0.2$ and $t = 2$.

5. Conclusion

In this flow model, generalized thermal and mass transport for the viscous fluid in cylindrical domain by utilizing the Prabhakar-like fractional derivative are discussed. The governing equations for temperature, concentration, and velocity are solved via Laplace and Hankel transforms for the closed-form results of field variables. The effects of physical parameters over thermal, molecular, and momentum profiles are posted by sketching the some graphs of temperature, concentration, and velocity fields. Some key findings of this study are listed below:

(1) Temperature, concentration, velocity profiles are enhanced for the increasing values of fractional parameter β for short time while showing a decreasing trend for large time.

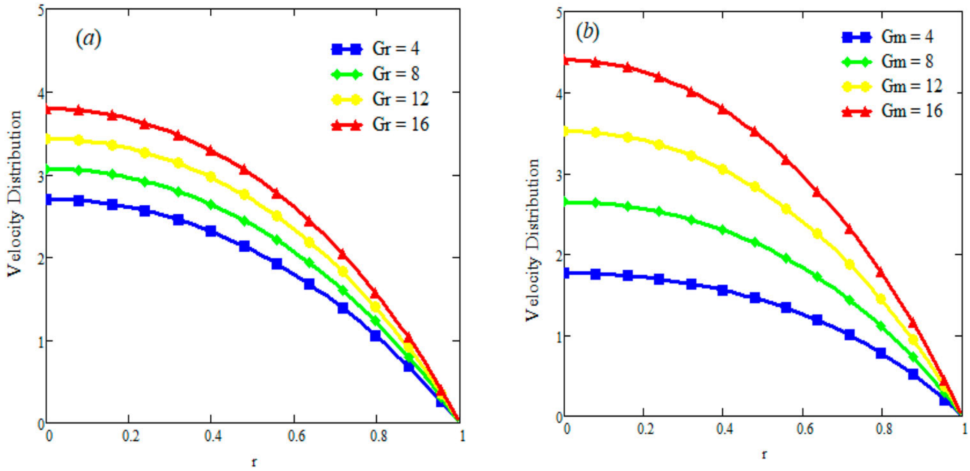

Figure 8. Velocity profile due to Gr and Gm variations.

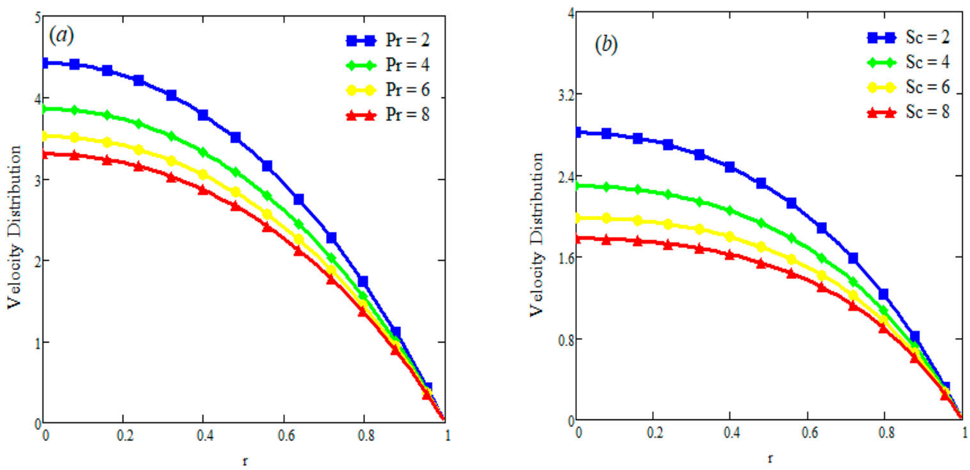

Figure 9. Velocity profile due to Pr and Sc variations.

(2) Temperature, concentration, and velocity profiles are lowered down for the increasing values of γ for both long and short times.
(3) Velocity profile is an increasing function for both thermal and mass Grashof numbers Gr and Gm respectively.
(4) Velocity profile is a decreasing function for the Prandtl number Pr and Schmidt number Sc.
(5) The generalized results for temperature, concentration, and velocity obtained with Prabhakar-like fractional derivative are of more decaying nature as compared to the other fractional derivatives.

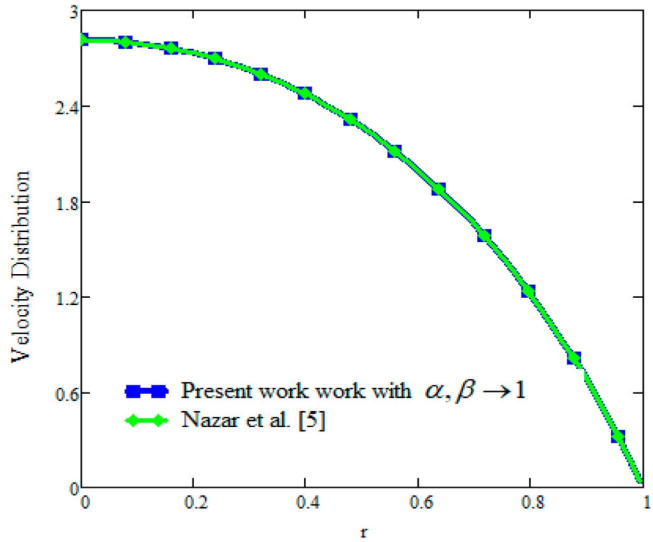

Figure 10. Comparison of this study with Nazar et al. [5].

The three-parametric Mittag–Leffler function is taken as the kernel for Prabhakar-like fractional derivative. As three-parametric Mittag–Leffler function is the generalization exponential function so our results for temperature, concentration, and velocity are more general results.

Disclosure statement

No potential conflict of interest was reported by the authors.

Funding

The authors are thankful to Higher Education Commission (HEC) Pakistan for facilitating this research.

References

[1] Jamil M, Fetecau C. Helical flows of Maxwell fluid between coaxial cylinders with given shear stresses on the boundary. Nonlinear Anal Real World Appl. 2010;11(5):4302–4311.
[2] Mahmood A, Parveen S, Ara A, et al. Exact analytic solutions for the unsteady flow of a non-Newtonian fluid between two cylinders with fractional derivative model. Commun Nonlinear Sci Numer Simul. 2009;14(8):3309–3319.
[3] Awan AU, Athar M, Imran M, et al. Exact analytical solutions for a longitudinal flow of a fractional Maxwell fluid between two coaxial cylinders. J Math. 2013;45:1–15.
[4] Aleema M, Imran MA, Chowdhury SR, et al. Analysis of mathematical model of fractional viscous fluid through a vertical rectangular channel. Chinese J Phys. 2019;61:336–350.
[5] Nazar M, Fetecau C, Awan AU. A note on the unsteady flow of a generalized second grade fluid through a circular cylinder subject to a time dependent shear stress. Nonlinear Anal Real World Appl. 2010;11(4):2207–2214.
[6] Nazar M, Sultan Q, Athar M, et al. Unsteady longitudinal flow of a generalized Oldroyd-B fluid in cylindrical domains. Commun Nonlinear Sci Numer Simul. 2011;16(7):2737–2744.

[7] Tong D, Shan LT. Exact solution for generalized Burger's fluid in an annular pipe. Meccanica. 2009;44(4):427–431.
[8] Shaowei W, Mingyu X. Axial Coutte flow of two kinds of fractional viscoelastic fluids in an annulus. Nonlinear Anal Real World Appl. 2009;10(2):1087–1096.
[9] Gul T, Akbar R, Zaheer Z, et al. The impact of the Marangoni convection and magnetic field versus blood-based carbon nanotube nanofluids. Proc Inst Mech Eng N J Nanomater Nanoeng Nanosyst. 2020;234(1–2):37–46.
[10] Oldham KB, Spanier J. The fractional calculus: theory and applications of differentiation and integration to arbitrary order. New York, NY: Academic Press; 1974. (Mathematics in Science and Engineering, Vol. 11).
[11] Podlubny I. Fractional differential equations. San Diego, CA: Academic Press; 1999. (Mathematics in Science and Engineering, Vol. 198).
[12] Hilfer R. Applications of fractional calculus in physics. Singapore: World Scientific Publishing; 2000.
[13] Elnaqeeb T, Shah NA, Mirza IA. Natural convection flows of carbon nanotubes nanofluids with Prabhakar-like thermal transport. Math Methods Appl Sci. 2020;1–14.
[14] Shah NA, Fetecau C, Vieru D. First general solutions for unsteady unidirectional motions of rate type fluids in cylindrical domains. Alex Eng J. 2018;57(3):1185–1196.
[15] Prakash J, Ogulu A. A study of pulsatile blood flow modeled as a power law fluid in a constricted tube. Int Commun Heat Mass Transf. 2007;34(6):762–768.
[16] Saqib M, Khan I, Shafie S. Generalized magnetic blood flow in a cylindrical tube with magnetite dusty particles. J Magn Magn Mater. 2019;484:490–496.
[17] Imran MA, Tahir M, Javaid M, et al. Exact solutions for unsteady flow of a fractional Maxwell fluid through moving co-axial circular cylinders. J Comput Theor Nanosci. 2016;13(5):3405–3413.
[18] Imran MA. Taylor–Couette flow of an Oldroyd-B fluid in an annulus subject to a time-dependent rotation. Am J Appl Math. 2015;3(3):25–31.
[19] Raza N, Haque EU, Rashidi MM, et al. Oscillating motion of an Oldroyd-B fluid with fractional derivatives in a circular cylinder. J Appl Fluid Mech. 2017;10(5):1421–1426.
[20] Ionescu C, Lopes A, Copot D, et al. The role of fractional calculus in modeling biological phenomena: a review. Commun Nonlinear Sci Numer Simul. 2017;51:141–159.
[21] Ali F, Imtiaz A, Khan I, et al. Flow of magnetic particles in blood with isothermal heating: a fractional model for two-phase flow. J Magn Magn Mater. 2018;456:413–422.
[22] Zokri SM, Arifin NS, Mohamed MKA, et al. Influence of viscous dissipation on the flow and heat transfer of a Jeffrey fluid towards horizontal circular cylinder with free convection: a numerical study. Mal J Fund Appl Sci. 2018;14(1):40–47.
[23] Vieru D, Siddique I. Axial flow of several non-Newtonian fluids through a circular cylinder. Int J Appl Mech. 2010;2(03):543–556.
[24] Sharma S, Singh U, Katiyar VK. Magnetic field effect on flow parameters of blood along with magnetic particles in a cylindrical tube. J Magn Magn Mater. 2015;377:395–401.
[25] Tzirtzilakis EE. A mathematical model for blood flow in magnetic field. Phys Fluids A. 2005;17(7):077103.
[26] Shah NA, Awan AU, Khan R, et al. Free convection Hartmann flow of a viscous fluid with damped thermal transport through cylindrical tube. Chinese J Phys. 80, 2022;45–61.
[27] Zheng L, Zhang X. Exact analytical solutions for fractional viscoelastic fluids. Model Anal Mod Fluid Probl. 2017;279–359.
[28] Ahmed N, Shah NA, Vieru D. Natural convection with damped thermal flux in a vertical circular cylinder. Chinese J Phys. 2018;56(2):630–644.
[29] Imran MA et al.. Applications of non-integer Caputo time fractional derivatives to natural convection flow subject to arbitrary velocity and Newtonian heating. Neural Comput. Appl. 2018; 30;1589–1599.
[30] Fetecau N.A. Shah C, Vieru D. General solutions for hydromagnetic free convection flow over an infinite plate with Newtonian heating, mass diffusion and chemical reaction. Commun Theor Phys. 2017;68(6):768–777.

[31] Debnath L, Bhatta D. Integral transforms and their applications. 2nd ed. Chapman & Hall/CRC; 2007.
[32] Piessens R. The Hankel transform, the transforms and applications handbook. 2nd ed. Boca Raton, FL: CRC Press LLC; 2000.
[33] Haubold HJ, Mathai AM, Saxena RK. Mittag–Leffler functions and their applications. J Appl Math. 2011;2011:1–51.